Science and Technology Journal Vol. 10 Issue: 1 January 2022 ISSN: 2321-3388

UWB BPF Using Hybrid Microstrip CPW with DGS Structure for Future Wireless Communication

Jagadish Baburao Jadhav[1*], Sagar Arun More[2], Vijay Shrinath Patil[3], Kiran Hilal Sonawane[4], Vaishali B Patil[5], Pravin Sahebrao Patil[6]

[1, 2, 3, 4] Department of Electronics and Telecommunication Engineering. R. C. Patel Institute of Technology, Shirpur-425405, India.

[5]Department: Master of Computer Applications. R. C. Patel Educational Trust's, Institute of Management Research and Development, Shirpur-425405, India.

[6]Department of Electronics and Telecommunication Engineering. S. S. V. P. S. B. S. Deore COEngineering, Dhule-424005, India.

[*]Email: jagadish.jadhav@rcpit.ac.in, jagadish.rcpit@gmail.com

Abstract—The aim of this paper is to design Ultra-Wide Band (UWB) Band Pass Filter (BPF) based on the microstrip-to-Coplanar Waveguide (CPW) transitions. UWB BPF using hybrid microstrip CPW and Defected Ground Structure (DGS) have been proposed and developed. Till now, few techniques are invented for designing UWB bandpass filter. One amongst these techniques is Hybrid Structure of two different planar transmission lines i.e. microstrip and coplanar waveguide are used. Compactness can be achieved by using this technique. A more flexible structure in terms of geometrical dimensions for getting optimum performance are obtained for planar circuit implementation. This is feasible thanks to the simultaneous use of microstrip and coplanar waveguide technologies. These qualities makes this technique superior over the other techniques. A detail experimental work of UWB B is presented in this paper. Alongside, the design and analysis of three (design 1, design 2 and design 3) UWB BPF structures is carried out. The UWB bandpass filter design gives a return loss less than -20 dB, flat group delay, very less insertion loss at every frequency point within whole UWB. These filter are useful alternative to other recently proposed structures in the literature.

Keywords: Coplanar Waveguide (CPW), Bandpass Filter (BPF), Coplanar Waveguide (CPW), Insertion Loss, Return Loss, Electromagnetic coupling, Defected Ground Structure (DGS), Transmission Zeros (TZs).

INTRODUCTION

Federal Communication Commission (FCC) sanctioned the unlicensed use of frequency band starting from 3.1 GHz to 10.6 GHz as Ultra-Wideband (UWB). For commercial communication applications in February 2002, the UWB radio system has been receiving great attention and gaining momentum from both academy as well as industry. A major device among many passive components is a bandpass filter design. In (Zhang et al. 2019) Five BPF is used to obtain UWB design by increasing or decreasing BPF in parallel according to requirement for electromagnetic acoustic signal detection. In (Bohra et al. 2020) a single notch band BPF with & without DGS technology is used which includes a pair of spiral shaped & H- slot resonators which gives good results. In (Raghava et al. 2021) proposed planer UWB BPF with two transmission zeros & DGS with complimentary split ring resonator & complementary folded split ring resonator. In (Karimi et al. 2019) designed compact narrow BPF in which two independently fully controllable passbands are used using two different coupling paths, got good simulation & measured results at 3.5 & 5.8 GHz with FBW 0.8% & 1%. In (Ghazali et al. 2018) a compact dual notch band UWB BPF is discussed. BPF is designed using microstrip to CPW

 https://doi.org/10.22232/stj.2022.10.01.09

technology. CPW is short circuited at ground & vertically connected to microstrip lines through dielectric. In (Wu et al. 2021) Nine high performance resonant modes are generated using direct connected T- shaped stub loaded resonator with three bands having FBW 65%, 42% and 31% and return loss of 42.9, 44.5 and 42.9 decibal. In (Sakotic et al. 2017) UWB BPF designed using circular patch resonator grounded via and unsettled by slits and DGS. This design is simulated, fabricated and measured, got outperforms compared with other UWB filters. In (Ghazali et al. 2017) broadside coupling of microstrip and coplanar waveguide is used. CPW is embedded in ground plane so that gives equispace resonant modes in UWB range. Four open ended stubs are appended on top to improve the performance. In (Bakali et al. 2020) microstrip coplanar waveguide microstrip transition is used, which gives good agreement between measurement and simulation results. In (Bakali et al. 2019) low budget FRP-4 is used, a flat group delay performance was obtained with variation of 0.15nS over the bandwidth suitable for wireless UWB devices as in (Bakalia et al. 2020) group delay about 0.22nS. In (Luo et al. 2010) a quasi-elliptic response and multi-mode UWB performance are obtained through DMR and transition from microstrip to CPW, mode stepped impedance resonator is used in (Wu et al. 2019). To obtain novel results a contiguous and concentric split ring resonators and ring resonators are used in (Mukherjee et al. 2017). A sharp out of band rejection performance is achieved in (Guo et al. 2015), triple mode stepped impedance resonator (Liu et al.2018) gives advantage to higher degree of freedom to adjust resonant frequencies. In (Gupta et al. 2017) triple notch UWB filter is designed using short circuit stubs and defected microstrip line structure. In (Hao et al. 2010), a wide array of novel and creative techniques to design an UWB bandpass filter is being reported. Fractional bandwidth is defined as absolute bandwidth divided by the center frequency. The fractional bandwidth is a better measure for bandwidth when comparing different antennas and filters because it is independent of scale:

$$Bf = 2\left(\frac{fh - fl}{fh + fl}\right) \quad (1)$$

Where fh is higher cutoff frequency and fl is lower cutoff frequency of passband. Normally this is defined as the range of the frequencies over which the return loss is acceptable. The detail literature can be seen from (Jadhav et al.2017).

Major contributions of this paper are:

1) Authors improved the Return loss (S_{11}).
2) Insertion loss (S_{21}) parameters of the filter, with DGS.
3) The parameters extraction using mathematical modelling of symmetrical networks for even mode and odd mode.
4) The design 1, design 2 and design 3 of UWB BPF structures with DGS exhibit a simple planar structure, compact size, resonance modes within the passband as well as independent of ground plane size and radiation pattern without supplementary circuit space.

The simulation results coming very good as Return loss S_{11} is flat to 20 dB, previously compaired to without DGS. The simulation results of (design 1, design 2 and design 3) UWB BPF structures with DGS are coming very good as Return loss S_{11} is steady and consistent to 20 dB. Such filters are suitable for use in (Jadhav et al.2017).

DESIGN 1: UWB BPF BASED ON HIGH PASS FILTER PROTOTYPE

The microstrip-to CPW transition arrangement in Figure 2 is adjusted to build a changeover stub of dimension w4, as shown in Figure 2. The dimensions for Figure 2 can be seen from the calculations: d1 = 0.038 cm, d2 = 0.05 cm, d3 = 0.0635 cm, and d4 = 0.028 cm. w1 = 8.9 cm, w2 = 0.381 cm, w3 = 0.559 cm, w4 = 0.0635 cm, w5 = 0.038 cm, w6 = 0.152 cm, and w7 = 0.521 cm.

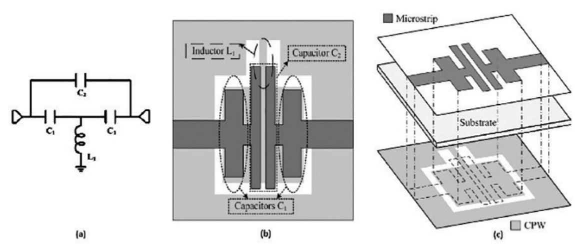

Fig. 1: (a) HPF Prototype with Capacitor C_2 (b) HPF Realized with Microstrip and CPW (c) 3-D View.

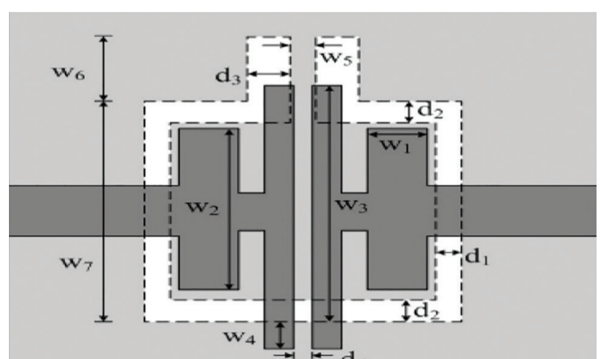

Fig. 2: Circuit Arrangements of Three-Pole UWB Bandpass Filter with Dimensions.

Design 1: Analysis of Symmetrical Network

As the circuit is symmetrical, even-odd mode investigation technique can be used to analyze the circuit. So, bisecting the circuit into two identical halves acting as a single port network individually. The bisected circuit diagram is shown in Figure 3.

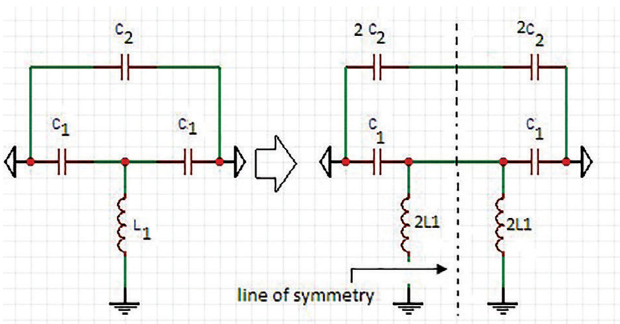

Fig. 3: Symmetrical Network.

Under even mode, line of balance acts as an open circuit as shown in Figure 4(a). Hence, capacitor C_2 will be disconnected from circuit.

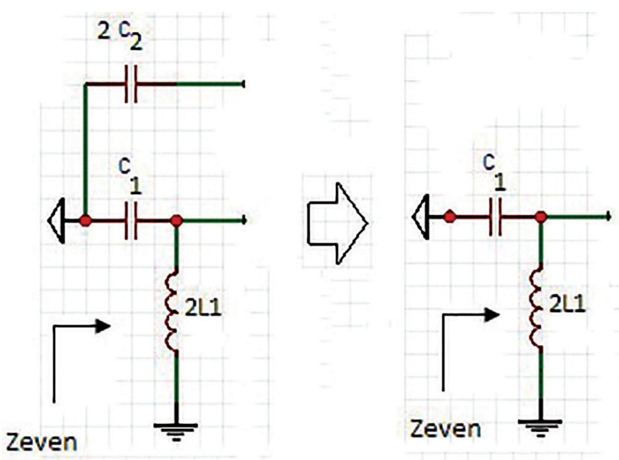

Fig. 4: (a) Even Mode Impedance (b) Odd Mode Impedance of Symmetrical Network.

This Even & Odd symmetric circuit decomposition technique removes the basic need for the RF designer to perform further simulations to obtain the even-mode and odd-mode circuits once the complete circuit S-parameters are known (Roberg et al. 2013). Conventionally Z_{even} and Z_{odd} are computed using equation given below.

$$Z_{even} = R + jX \tag{2}$$

$$Z_{even} = 0 + j\,(X_L - X_C) \tag{3}$$

$$Z_{even} = j\,(2wL_1 - 1/wC_1) \tag{4}$$

Underneath odd mode, line of symmetry acts as a short circuit as shown in 4.4(b). Hence, capacitor L_1 will be shorted.

$$Z_{odd} = R + jX \tag{5}$$

$$Z_{odd} = 0 + j(X_L - X_C) \tag{6}$$

$$Z_{odd} = (1/jw\,(C_1 + 2C_2)) \tag{7}$$

A transmission zero is produced when the transfer function S_{21} is identical to zero, i.e.

$$Z_{even} = Z_{odd} \tag{8}$$

The width of input and output microstrips are calculated in a way so that the microstrips can have a characteristics impedance of 50 ohm in order to have a proper impedance matching when used in application circuit. Substrate height is taken equal to 0.508 mm and dielectric constant of 3.38. Thus using this data and equation, effective dielectric constant and characteristics impedance are calculated. The thickness of input as well as output microstrips is designed for the characteristics impedance to be 50Ω. The calculated width is 1 mm.

Design 1: Simulation Result

Mentor graphics HyperLynx IE3D electromagnetic simulator is used for design, edit and simulation purpose. IE3D software uses method of moments for analysis of structure (Mentor Graphics Manual 2020). The scattering parameters i.e. S-parameters are used to analyze the filter performance. Transmission coefficient is characterized by insertion loss (S_{21}) and reflection coefficient is characterized by return loss i.e. (S_{11}). The S-parameter graph is shown in Figure 5. The 10 dB bandwidth is from 3.29 GHz to 8.00 GHz. Thus the passband width is 4.71 GHz. The fractional bandwidth is 78.5%. Figure 6 shows current distribution of design 1. Current is flowing through the filter structure with 18 dB loss. The in-band return and insertion losses are good (i.e.$|S_{11}| \geq -20$ dB, and $|S_{21}| \leq -1$ dB) with frequency selectivity at both edges is high. The green line indicates the S_{21} and other colour line indicates the S_{11} as shown in Figure 5. The practical S_{11} and S_{21} response shows even better agreement with the calculation.

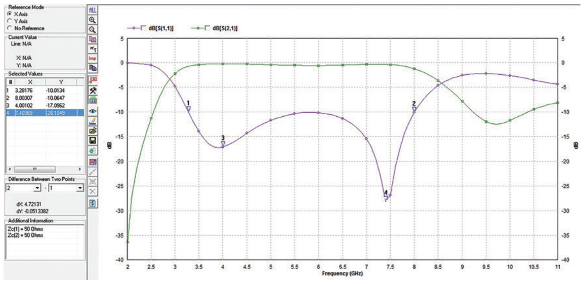

Fig. 5: Simulation Results of S-Parameters S_{11} Vs. Operating Frequency of Design 1.

Figure 7 shows group delay of design 1. Group delay is constant in the UWB. The filter reported in design 1 has very good selectivity. Poles has been seen at the start of UWB and at the end of UWB to improve the selectivity of the filter.

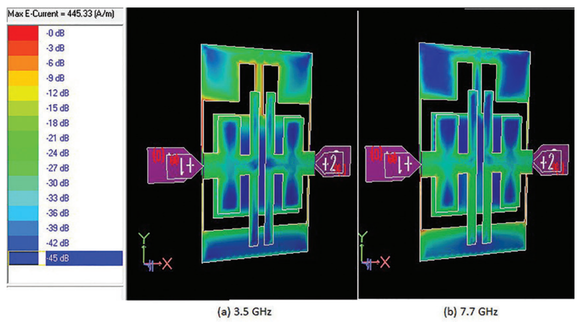

Fig. 6: Simulation Results of Current Distribution Vs. Operating Frequency of Design 1.

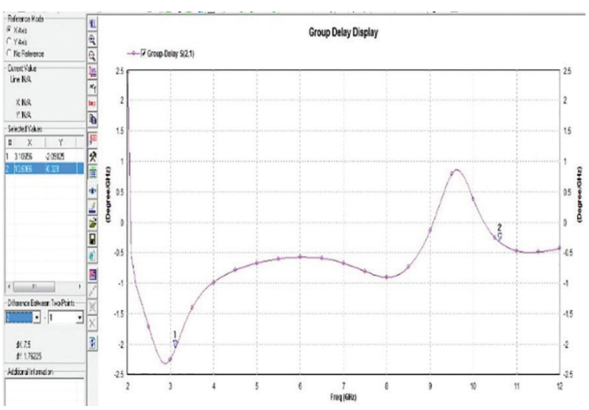

Fig. 7: Simulation Results of Group Delay Vs. Operating Frequency of Design 1.

DESIGN 2: UWB BPF WITH

MULTIPLE RESONATING STRUCTURE

A CPW non uniform resonator or multiple-mode resonator (MMR) is created. In this design, the UWB filter is designed by taking substrate of relative dielectric constant of 10.8 and thickness of 0.635 mm.

Table 1: Frequencies of Resonance are Determined (f1, f2, f3) with (S1) for the Multi-Mode Resonator in Figure 9.

S1	0.18	0.58	0.98	1.10	1.38	1.78
$f1(GHz)$	3.67	4.01	4.12	4.13	4.15	4.16
$f2(GHz)$	7.29	7.10	6.84	6.76	6.60	6.34
$f3(GHz)$	10.91	10.12	9.55	9.40	9.13	8.74

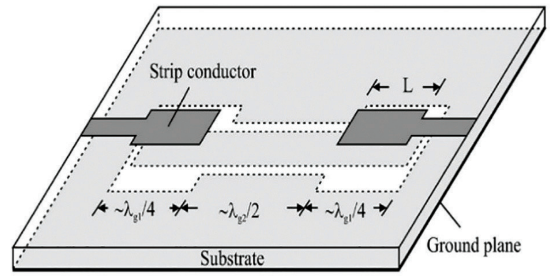

Fig. 8: Schematic of UWB BPF (Design 2).

Figure 9(a) shows, the open-ended multi-mode resonator. Figure 9(b) shows its equivalent circuit. Here, Yi = 0 for calculations of resonant modes frequencies. Figure 10(a) shows a hybrid microstrip/CPW surface-to-surface connection. Its coupling may emphasized in terms of a parallel J-inverter series as illustrated in Figure 10(b). The three stubs in CPW are grounded to the common ground of CPW. There are two microstrip open-circuited stubs on top side of common substrate. These microstrip open-circuited stubs are separated by a gap g1. A vertical coupling between top microstrip stub and bottom CPW side stubs is achieved. The dimensions for the structure are shown in figure 10.

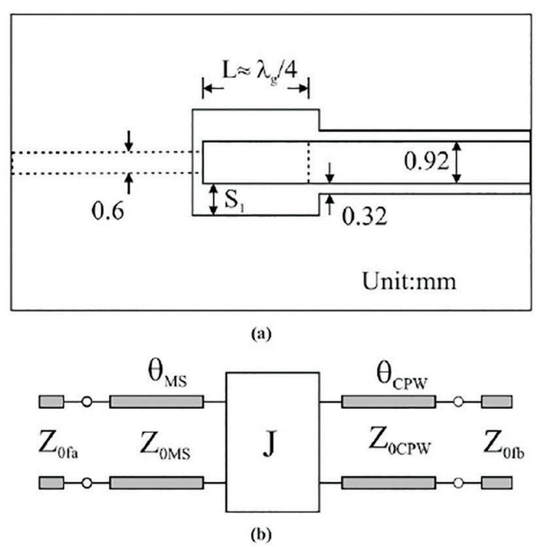

Fig. 9: MMR on Coplanar Waveguide Transition (a) Design. (b) Corresponding Network.

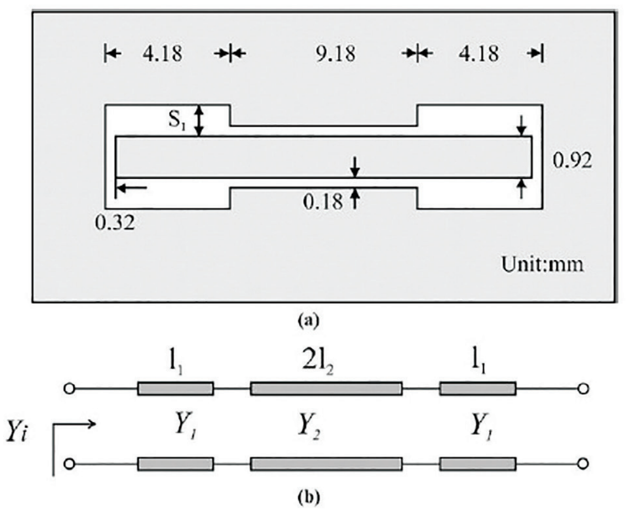

Fig. 10: Layout of Microstrip/CPW Connection (a) Design with Dimensions. (b) Corresponding J-Inverter Setup.

DESIGN 2: SIMULATION RESULT

The insertion loss is flat and closer to 0-dB line and return loss is below -10 dB line as shown in Figure 11. The 10 dB bandwidth starts from 2.99 GHz to 10.55 GHz. The width of passband is (10.55-2.99) = 7.56 GHz. The FBW is 111.69%. The filter structure in design 2 gives five transmission poles. The electromagnetic simulation software used for designing and simulating the filter structure is Mentor Graphics Hyperlynx IE3D (Mentor Graphics Manual 2020). It uses the method of moment to analyse the structure. Figure 3 shows how a filter structure looks in IE3D Mgrid editor. The yellow part shows open-circuited microstrip stubs and green part shows CPW. The finite ground plane provided by IE3D is used for designing and simulating the filter. So, differential ports are deployed for input output. The simulation results are shown in Figure 4. The transmission response i.e. insertion loss is predicted from S_{21} and return loss is predicted from S_{11}. As can be seen from results, five transmission poles are obtained within UWB. The S_{21} is very close to the 0 dB line within desired band that means insertion loss arised due to filter is very minimum. The S_{11} is staying below -15 dB line this means a negligible amount of power is reflecting back to the port. The in-band return and insertion losses are good (i.e. $|S_{11}| \geq -10$ dB, and $|S_{21}| \leq -1$ dB) with frequency selectivity at both edges is high. The green line indicates the S_{21} and other colour line indicates the S_{11} as shown in Figure 11.

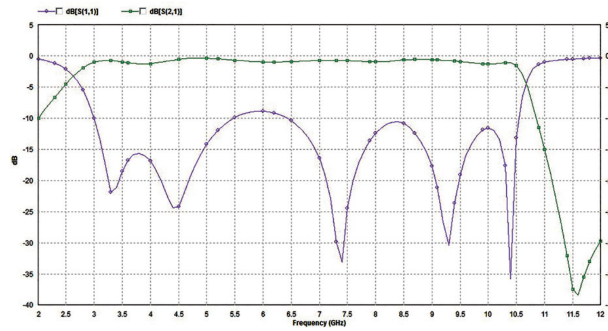

Fig. 11: Simulation Results of S-Parameters S_{11} Vs. Operating Frequency of Design 2.

The current distribution of design 2 is shown in Figure 12. The surface current spreading at 3.3, 4.4, 7.3, 9.2 and 10.3 GHz the surface current density is largely concentrated in the ground plane around the hybrid microstrip coplanar waveguide. The current is flowing through the filter at resonant frequencies with 12 dB loss which is negotiable. Group delay is shown in Figure 13 it ranges between 0.46 to 0.74 ns, with the peak deviation of 0.30 ns over the entire UWB passband.

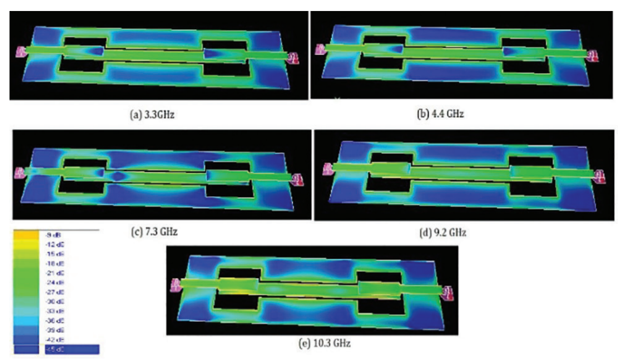

Fig. 12: Simulation Results of Current Distribution Vs. Operating Frequency of Design 2.

DESIGN 3: UWB BPF WITH CPW QUARTER WAVELENGTH RESONATOR

The top microstrip structure and bottom CPW structure are electromagnetically coupled for signal energy transfer from input port to output port. The central conducting strip of conventional coplanar waveguide is customized to get three stubs. In this way, three stubs are designed within coplanar waveguide. These stubs are having their length quarter of the guided wavelength at the center frequency. Among these three stubs, two side stubs are of equal length while the central stub has length shorter than the two side stubs as shown in Figure 13. The filter is designed with a substrate having relative dielectric constant of 3.05 and a depth of

0.0508 cm. Proper results can be obtained for the dimensions, W2 = 0.14 cmm, d1 = 0.02 cm, d2 = 0.06 cm, g1 = 0.24 cm. W0 = 0.12 cm, L1 = 0.62 cm, L2 = 0.88 cm, W1 = 0.08 cm, the substrate parameters for designing filter are dielectric constant ε = 3.38, thickness (h) = 0.508 mm, tan δ = 0.002. The width W0 is taken as 0.12 cm for getting 50 Ω impedance. It can be calculated using formula in (Jadhav et al.2017). It solely depends upon effective dielectric constant, thickness h of substrate. Using CPW multiple resonating structure, three transmission poles can be obtained and to make band as flat as possible, top open circuited microstrips are designed which in turn to lead a five pole structure as a whole.

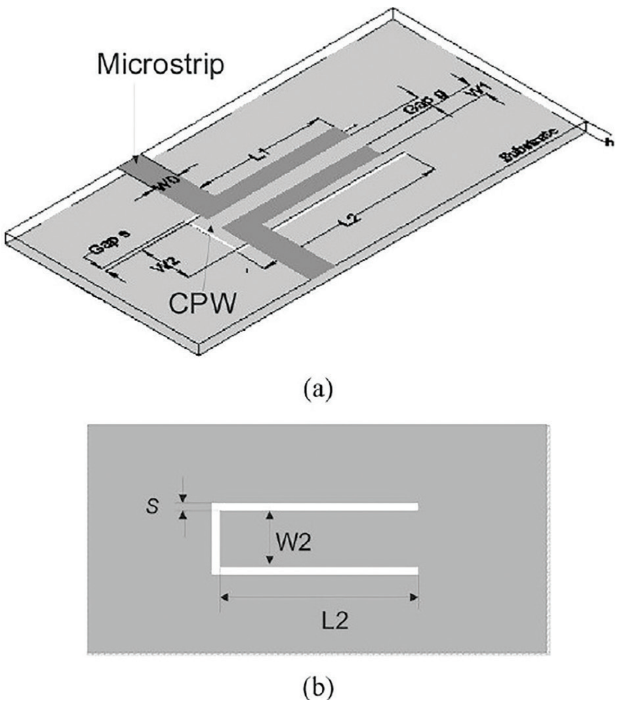

Fig. 13: Schematic of Design 3.

Design 3: Simulation Result

Figure 15 shows the simulation result of design 3. The BPF gives a FB of 90 percent at a center frequency of 5.4, as well as poles at 1.95 and 10.36. The proposed filter can find the application in 5G and 6G tranreceiver front end design technology to achieve ubiquitous communications. Figure 16 shows current distribution at resonant frequencies. Figure 14 shows how a filter structure looks in IE3D Mgrid editor. The yellow part shows open-circuited microstrip stubs and green part shows CPW. The finite ground plane provided by IE3D (Mentor Graphics Manual 2020) is used for designing and simulating the filter. So, differential ports are deployed for input output. The simulation results are shown in Figure 15. The transmission response i.e. insertion loss is predicted from S_{21} and return loss is predicted from S_{11}. As can be seen from results, five transmission poles are obtained within UWB. The S_{21} is very close to the 0 dB line within desired band that means insertion loss arised due to filter is very minimum. The S_{11} is staying below -15 dB line this means a negligible amount of power is reflecting back to the port. Further changes in design can be made with the help of optimization. By deciding optimization parameters, optimum performance can be obtained using optimization process. Taking into account the constant technological advances in the field of wireless communication devices and services, we can further modify the proposed design by making changes in CPW structure. To achieve this, slots, DGS, quasilumped elements can be utilized.

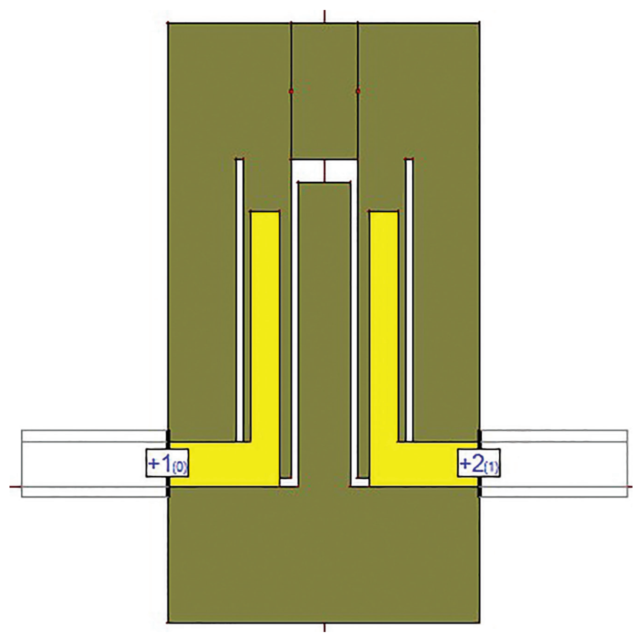

Fig. 14: UWB BPF Structure in IE3D MGRID Editor.

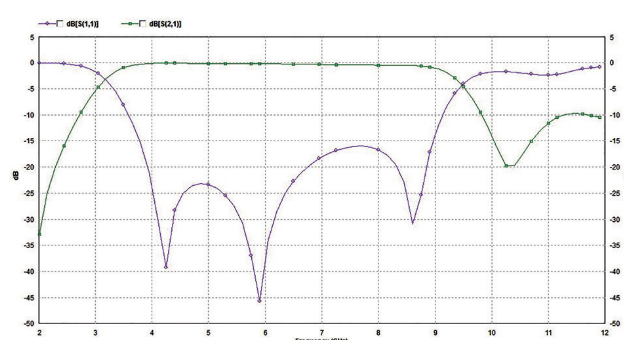

Fig. 15: Simulation Results of S-Parameters S_{11} Vs. Operating frequency of Design 3.

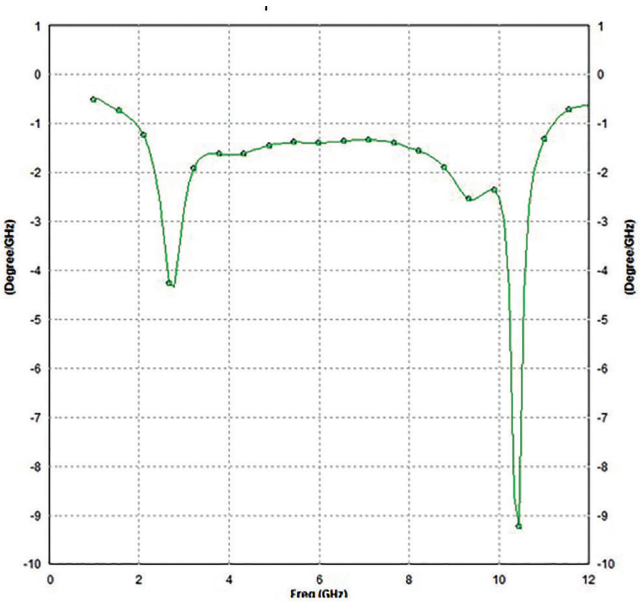

Fig. 16: Simulation Results of Group Delay Vs. Operating Frequency of Design 3.

The in-band return and insertion losses are good (i.e. $|S_{11}| \geq -10$ dB, and $|S_{21}| \leq -1$ dB) with frequency selectivity at both edges is high. The green line indicates the S_{21} and other colour line indicates the S_{11} as shown in Figure 15. Figure 16 shows group delay within whole UWB passband. A flat group delay. Coplanar waveguide structure is utilized to get multiple resonances and to make the band as flat as possible, quarter wavelength microstrip resonators are deployed. The simulation results shows good transmission characteristics, reflection characteristics and group delay within band of interest (Mentor Graphics Manual 2020). The transmission coefficient S_{21} is given as (Hao et al.2010, Hong et al. 2001).

$$S_{21} = \frac{\left(Z_{even} - Z_{odd}\right)Z_0}{\left(Z_{even} + Z_0\right)\left(Z_{odd} + Z_0\right)} \tag{9}$$

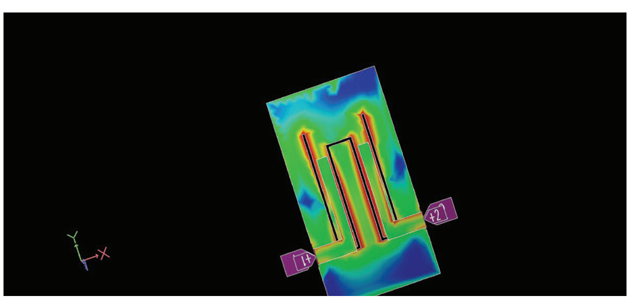

Fig. 17: Simulation Results of Current Distribution Vs. Operating Frequency of Design 3.

CONCLUSION

The UWB technology will be the more popular for high speed wireless communication and it will provide key solution for the future wireless personal area network (WPAN) systems and is gaining momentum. A detail experimental work of UWB bandpass filter is presented in this study. Alongside, the design and analysis of three (design 1, design 2 and design 3) UWB BPF structures is carried out. The UWB bandpass filter of design 1 gives a return loss less than -20 dB, flat group delay, very less insertion loss at every frequency point within whole UWB. In design 1 The 10 dB bandwidth is from 3.29 GHz to 8.00 GHz. Thus the passband width is 4.71 GHz. The fractional bandwidth (FB) is 78.5%. In design 2 The 10 dB bandwidth starts from 2.99 GHz to 10.55 GHz. The width of passband is (10.55-2.99) = 7.56 GHz. The FBW is 111.69%. The filter structure in design 2 gives five transmission poles. In design 3 the BPF gives a FB of 90 percent at a center frequency of 5.4, as well as poles at 1.95 and 10.36. The proposed filter can find the application in 5G and 6G tranreceiver front end design technology to achieve ubiquitous communications. The proposed UWB BPF has improved return loss performance i.e. -20 dB at every frequency within UWB. The insertion loss due to filter is very less. The size of filter is compact and suitable for UWB applications where compactness is an important design constraint.

REFERENCES

A. Kamma, J. Mukherjee (2017) Multiple band notch and Dual-Band filter using concentric and contiguous split ring resonators (CCSRR), Journal of Electromagnetic Waves and Applications, 31(1):57-71.

Abu Nasar Ghazali, Mohd Sazid, Srikanta Pal (2018) Dual band notched UWB-BPF based on hybrid microstrip-to-CPW transition AEU - International Journal of Electronics and Communications, Volume 86:55-62.

Abu NasarGhazali, MohdSazid, SrikantaPal (2017)A compact broadside coupled dual notched band UWB-BPF with extended stopband AEU - International Journal of Electronics and Communications 82:502-507.

D. M. Pozar (1998) Microwave Engineering 2nd ed. New York: Wiley.

Gholamreza Karimi, YeganehPourasad, AliLalbakhsh, HesamSiahkamari (2019) Design of a compact ultra-narrow band dual band filter for WiMAX applicationAEU - International Journal of Electronics and Communications 110:1-5.

H. El Omari El Bakali, H. Elftouh, A. Farkhsi, A. Zakriti, M. El Ouahabi (2020) Design of a Super Compact UWB Filter Based on Hybrid Technique with a Notch Band Using Open Circuited Stubs AEM Journal 9(3):39-46.

Hamza el Omari el Bakali (2019) Design of a Compact UWB BPF Using a Hybrid Structure and a Staircase-Shaped DGS International Journal of Microwave and Optical Technology 14(5):306-313.

Hamza El Omari El Bakalia, Hanae Elftouha , Abdelkrim Farkhsia , Alia Zakritib (2020) A Compact UWB Bandpass Filter with WLAN Band Rejection Using Hybrid Technique Elsevier B.V. 46:922-926.

He Zhu, Sai Wai Wong, Shenjie Wen, and Qing Xin Chu (2013) An Ultra-wideband (UWB) Bandpass Filter with Microstrip-to-CPW Transition and a Notch-band IEEE.

Hussain Bohra; Amrit Ghosh; Anand Bhaskar; Arvind Sharma (2020) A Miniaturized Notched Band Microstrip Wideband Filter with Hybrid Defected Ground Structure Technique published in Third IEEE International Conference on Smart Systems and Inventive Technology (ICSSIT) 745-750.

J. S. Hong and M. J. Lancaster (2001)Microstrip Filters for RF/ Microwave Applications New York: Wiley.

Jagadish B Jadhav and Pramod J Deore (2017) A compact planar ultra-wideband bandpass filter with multiple resonant and defected ground structure AEU - International Journal of Electronics and Communications 81:31-36.

Jagadish Baburao Jadhav, Pramod Jagan Deore (2017) Filtering antenna with radiation and filtering functions for wireless applications," Journal of Electrical Systems and Information Technology 4(1):125-134.

Jia-Kang Wu, Jun-Ge Liang, Xiao Wang, Nam-Young Kim, Xiaofeng Gu (2021) Multi-band bandpass filter based on direct-connected T-shaped stub-loaded resonator.

L. Wu, P. Hu, C. Li, L. Li, C. Tang (2019) A Novel Compact Microstrip UWB BPF with Quad Notched Bands Using Quad-Mode Stepped Impedance Resonator, Progress In Electromagnetics Research Letters 83:51–57.

M. Roberg and C. Campbell (2013) A Novel Even & Odd-Mode Symmetric Circuit Decomposition Method IEEE Compound Semiconductor Integrated Circuit Symposium (CSICS) 1-4.

Mentor Graphics HyperLynx IE3D electromagnetic simulator Manual 2020.

Mohd Sazid N.S.Raghava (2021) Planar UWB-bandpass filter with multiple passband transmission zeros AEU - International Journal of Electronics and Communications 134.

Rainee N. Simons (2001) Coplanar Waveguide Circuits, Components and Systems John Wiley & Sons, Inc.

S. C. Gupta, M. Kumar, R. S. Meena (2017)Design and Analysis of Triple Notched Band Uwb Band Pass Filter Using Defected Microstrip Structure (Dms), International Journal of Wireless Communications and Mobile Computing 5(6):32-44.

Tian-xiang Hu; Ying-hong Zhang; Xiao Wei; Zheng-hua Qian (2019) Design of an Ultra-Wideband Band-Passfilter Circuit for Electromagnetic Ultrasonic Signal Condition 13th Symposium on Piezoelectrcity, Acoustic Waves and Device Applications (SPAWDA).

Vikram Sekar and Kamran Entesari (2011) Miniaturized UWB Bandpass Filters With Notch Using Slow-Wave CPW Multiple-Mode Resonators IEEE Microw. Wireless Compon. Lett., 21 (2):80-82.

X. Guo, Y. Xu, W. Wang (2015) Miniaturized Planar Ultra-Wideband Bandpass Filter with Notched Band, Journal of Computer and Communications 3:100-105.

X. Liu, C. Zhong, H. Song, Y. Chen, T. Luo (2018) A New Compact Microstrip UWB Bandpass Filter with Triple-Notched Bands and Good Stopband Performance, Progress In Electromagnetics Research Letters 72:29–37.

X. Luo, J.-G. Ma, K. Ma, and K. S. Yeo (2010) Compact UWBbandpass filter with ultra narrow notched band IEEE Microw. Wireless Compon. Lett., 20 (3):145–147.

ZarkoSakotic, Vesna Crnojevic-Bengin Nikolina Jankovic(2017) Compact circular-patch-based bandpass filter for ultra-wideband wireless communication systems AEU - International Journal of Electronics and Communications 82.

Zhang-Cheng Hao and Jia-Sheng Hong (2010) Ultrawideband Filter Technologies IEEE Microw. Mag., 56-68.